Journal of Cleaner Production 406 (2023) 137069

Contents lists available at ScienceDirect

Journal of Cleaner Production

journal homepage: www.elsevier.com/locate/jclepro

An innovative spinning process for production and characterisation of ring-spun hybrid yarns from recycled carbon fibre

Beatrice Colombo [a,b,*], Paolo Gaiardelli [a], Stefano Dotti [a], Flavio Caretto [b]

[a] Department of Management, Information and Production Engineering, University of Bergamo, Viale Marconi 5, 24044, Dalmine (BG), Italy
[b] Division for Sustainable Materials, ENEA - Italian National Agency for New Technologies, Energy and Sustainable Economic Development, Brindisi Research Center, SS7 Appia Km 706,00, Brindisi (BR), 72100, Italy

ARTICLE INFO

Handling Editor: Yang Liu

Keywords:
Recycled carbon fiber
Innovative spinning process
Ring spinning
Hybrid yarns
Mechanical properties
Sustainability

ABSTRACT

The growing focus on sustainability stresses the importance of using materials derived from manufacturing scraps and end of life. Nowadays, a large amount of carbon fibre waste is available, and therefore, it is pivotal to understand how to use it for value-added applications. This paper introduces an innovative spinning process for ring-spun hybrid yarns composed of recycled carbon fibres (rCFs) from manufacturing scraps and virgin thermoplastic fibres in different blending ratios. The ultimate goal is to assess whether such a process is able to produce ring-spun hybrid yarns suitable for the production of polymer composites for structural applications and to determine the blends range that addresses this goal. The actual innovation in this process lies in the use of a ring-spinning machine for the production of hybrid yarns, which were characterised by tensile tests and thermogravimetric analysis combined with differential scanning calorimetry. The results show that the range of rCFs for the production of ring-spun hybrid yarns with good mechanical and thermal properties lies between 50% and 70%. Fibre orientation is crucial, especially for the card web, as is the blending ratio for the whole process. The increase in the number of draw frame doublings and the actual number of remaining rCFs have an impact on the tenacity of the hybrid yarn. Finally, ring-spun hybrid yarns consisting of 70% rCF exhibit slightly higher tensile strength, but with a lower decrease in the quantity of rCFs than those composed of 50% rCF. Thus, they possess the best mechanical and thermal properties and composites made from ring-spun hybrid yarns with 70% rCF should perform better. Overall, this process has the potential to be industrially transposed but needs to be evaluated from an environmental perspective.

1. Introduction

Carbon fibres (CFs) are a valuable material with remarkable physical, chemical and mechanical properties (Yao et al., 2018). They are adopted by companies for the production of carbon fibre-reinforced plastic (CFRP) composite materials, which, accordingly, exhibit outstanding mechanical properties, low weight, corrosion resistance and good fatigue behaviour (Clark et al., 2020; Tehrani et al., 2013). Owing to these characteristics, they are increasingly being used in several industries, such as the automotive, aircraft, luxury sports equipment and construction industries, in place of traditional materials, including aluminium or steel (Cousins et al., 2019; Lefeuvre et al., 2017; Liu et al., 2017). In 2018, the volume of global demand for CFRP was around 128.5 thousand tonnes, about 12.7% higher than the value achieved in the previous year and almost three times that obtained in 2010 (Sauer, 2019). This extensive use will imply huge amounts of waste, both from manufacturing processes (i.e. bobbin ends, selvedge and offcuts) and products' end of life (Pimenta and Pinho, 2011), that need to be managed. The overall CFRP waste is expected to increase to 20 kt per year by 2025 (Rademacker, 2018). Over the last few decades, this waste has mostly been incinerated or put in landfills (Pickering, 2006; Pimenta and Pinho, 2011) causing significant environmental issues and considerable economic losses for businesses (Colombo et al., 2021b; Naqvi et al., 2018). In light of sustainability, these disposal routes are becoming increasingly restrictive (Bernatas et al., 2021; Longana et al., 2021), and recycling options to recover CFs appear to be the best way

* Corresponding author. Department of Management, Information and Production Engineering, University of Bergamo, Viale Marconi 5, 24044, Dalmine (BG), Italy.
E-mail addresses: beatrice.colombo@unibg.it (B. Colombo), paolo.gaiardelli@unibg.it (P. Gaiardelli), stefano.dotti@unibg.it (S. Dotti), flavio.caretto@enea.it (F. Caretto).

https://doi.org/10.1016/j.jclepro.2023.137069
Received 12 December 2022; Received in revised form 23 March 2023; Accepted 1 April 2023
Available online 5 April 2023

forward to reduce environmental impacts as well as generate cost savings (Colombo et al., 2022; Fernández et al., 2021). On one hand, recycled carbon fibres (rCFs) require about 10% less energy consumption than virgin CFs to be produced (Witik et al., 2013) and, on the other hand, they are cheaper as they do not require the pricey precursors mandatory to obtain virgin CFs (for comparative purposes, the price of virgin CFs ranges from €17–50/kg, while the price of rCFs is around €8–12/kg) (Fernández et al., 2021). However, the recycling of CFRPs is often difficult to implement due to their heterogeneous nature (Pickering, 2006). Concurrently, existing reclamation technologies, namely pyrolysis, fluidised bed and solvolysis, do not currently allow the recovery of high-quality material due to the "fluffy" form (Longana et al., 2021; Yang et al., 2012). Therefore, currently, rCFs from any source of waste (i.e. manufacturing scraps and/or waste, prepreg residuals or waste and end of life CFRPs) are mainly adopted by companies for second-quality applications, including short fibre random mats (i.e. non-woven fabrics) (Hengstermann et al., 2017) and injection moulded composites (Hasan et al., 2018), suitable for non-structural applications including aircraft and vehicle interiors (Hengstermann et al., 2017). Indeed, such materials are generally characterised by low mechanical properties due to randomly oriented fibres, poor fibre content and high fibre damage during manufacturing (Pickering et al., 2016; Wölling et al., 2017).

To overcome these drawbacks and consequently expand the application of rCFs to more structural components, fibre alignment must be pursued (Such et al., 2014). Among pneumatic, electric field, ultrasonic and fluid-based methods, the highest degree of alignment seems to be provided by hydrodynamic techniques (Longana et al., 2021), including a rotating drum developed at the University of Nottingham (Wong et al., 2010), HiPerDiF from the University of Bristol and Lineat Composites (Longana et al., 2016) and TuFF process developed by the University of Delaware (Tierney et al., 2019).

Another method to improve fibre alignment that has attracted increasing interest from researchers is the spinning process (Akonda et al., 2012; Goergen et al., 2020; Hasan et al., 2018; Hengstermann et al., 2016) since yarns exhibit high fibre orientation and good compactness (Hasan et al., 2018; May et al., 2021). Accordingly, reinforcement composed of them could drastically improve CFRP performance. Nevertheless, the spinning of rCFs is not as well established as the spinning of traditional textile fibres (e.g. cotton, hemp and wool). CFs are brittle, sensitive to stresses and without natural crimp (Hengstermann et al., 2016), thus making the traditional spinning process unproductive and complex. In such a context, the necessity to readjust the traditional spinning process emerges as essential for fabricating yarns with repeatable physical, thermal and mechanical properties for structural applications (Hengstermann et al., 2021). However, few studies have been carried out to date on the production of hybrid yarns from CF staple waste (Pakdel et al., 2020). Specifically, these hybrid yarns have been produced using roving frame (Hengstermann et al., 2016, 2017), wrap spinning (Akonda et al., 2012, 2014; Goergen et al., 2020) and friction spinning (Hasan et al., 2018) technologies. In greater detail, Hengstermann et al. (2016) produced yarns made up of virgin CF cut to simulate the rCFs from manufacturing scraps of 40 and 60 mm length and polyamide 6. They found that the physical and mechanical properties of the obtained yarns are affected by fibre length, level of twist and fibre volume fraction within the yarn. Likewise, these parameters affected the tensile strength of the unidirectional composites produced, which was found to be around 771 and 838 MPa. Hengstermann et al. (2017), using the same fibres as the previous study but with a different content, noted that the mechanical properties of the composites are affected by yarn twist and fibre volume fraction. In such a context, a recent study by Abdkader et al. (2022) investigated the possibility of manufacturing hybrid yarns with low twist using a roving frame to improve composites' mechanical properties.

Furthermore, Akonda et al. (2012) used rCFs of around 50 mm length from thermal recycling and PP fibres with blending ratios of 30–70% and 50–50% by weight, respectively, to obtain hybrid yarns. The analysis of their mechanical properties highlighted that the blending ratio is crucial, as the greater the quantity and length of rCFs present, the higher is the tensile strength (Akonda et al., 2012). Goergen et al. (2020), using wrap spinning to produce hybrid yarns composed of waste CF and polyamide 6, discovered that recycled fibre-reinforced thermoplastic composites consisting of non-crimp fabrics have a maximum tensile strength of 805 MPa. Additionally, Hasan et al. (2018) manufactured core-sheath hybrid yarns consisting of 60 mm length rCFs as sheaths and polyamide 6 as the core by friction spinning. They found that the air suction needed when producing hybrid yarns and their core to sheath ratio influenced the mechanical properties of unidirectional thermoplastic composites. Overall, despite some technical drawbacks, the results found in previous investigations are promising (Khurshid et al., 2020). Nevertheless, these production methods do not ensure high-quality yarns, such as with ring spinning. Indeed, it is widely recognised that ring-spun yarns are of such quality as to be suitable for the manufacture of fabrics that can be applied to a wide range of end uses (Lawrence, 2003). Moreover, ring spinning enables the processing of not only most natural and man-made fibres but also fibre blends (Lawrence, 2003). This study's approach is guided by the consideration that the development of processes to achieve value-added products employing yarns is essential in light of the circular economy (Pakdel et al., 2020). Therefore, the present study takes its cue from a previous feasibility study (Colombo et al., 2021a) to propose an innovative spinning process for rCFs from manufacturing scraps and blended with thermoplastic fibres – referred to as *Innovative Spinning Process for Recycled Carbon Fibres (ISP4rCF)* – to produce ring-spun yarns for the production of CFRPs suitable for structural components at the laboratory level.

Based on this premise, this paper aims to introduce the ISP4rCF and assess the mechanical and thermal–physical properties of hybrid yarns produced on a ring spinning machine by varying the rCF weight content (i.e. 50% and 70%), the thermoplastic fibre (i.e. polyester and polyamide) and the number of draw frame doublings (i.e. 3 or 5). Tensile tests and thermogravimetric analysis combined with differential scanning calorimetry were carried out to allow comparison between the different ring-spun hybrid yarns obtained in view of their applications in CFRPs suitable for structural components. Overall, the novelty of this study concerns the possibility of producing yarns and semi-finished products composed of rCF that are suitable for structured reinforcements of good value-added on a ring spinning machine, thus fostering upcycling.

2. Materials

The rCFs used for this investigation were supplied by an Italian company specialising in the production of CF fabrics. The authors established to use CFs recovered as scraps from manufacturing, as this kind of waste represents the main source of CFRP waste, with about 40% of the total waste generated (Pickering, 2006; Pimenta and Pinho, 2011). Specifically, rCF of dry fabrics (unidirectional or weaving), already opened by the supplier through a mechanical process able to untangle the weft and warp threads or unidirectional wefts, was adopted. Thus, no pre-processing treatment was performed. Furthermore, precisely for this reason, from a technical perspective this type of rCF shows similar properties to virgin CFs (Hasan et al., 2018); therefore, it is supposed to be easier to process. The average length of rCF was declared by the provider to be 62 ± 5 mm. Polyester and polyamide fibres length was on average 60 mm to match the length of rCFs used in this study. Such virgin thermoplastic fibres were selected as carriers for rCFs due to their good fibre-to-fibre cohesion and entanglement (Akonda et al., 2014; Hengstermann et al., 2016). Indeed, rCFs are characterised by low fibre cohesion since they have a smooth surface and no crimps. Consequently, they do not allow for the production of a web with acceptable mechanical characteristics.

Because commercially available rCF typically contains fibres with

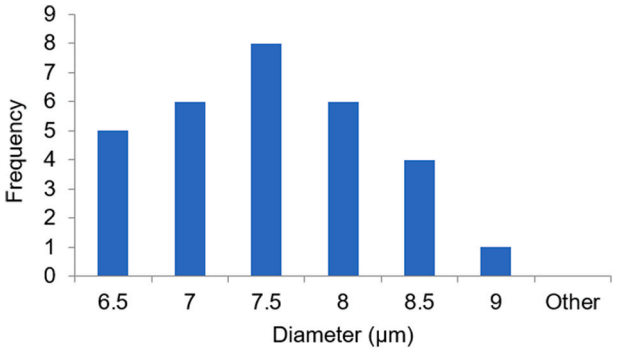

Fig. 1. Statistical distribution of the diameter of rCFs assessed with a sample of 30 measures.

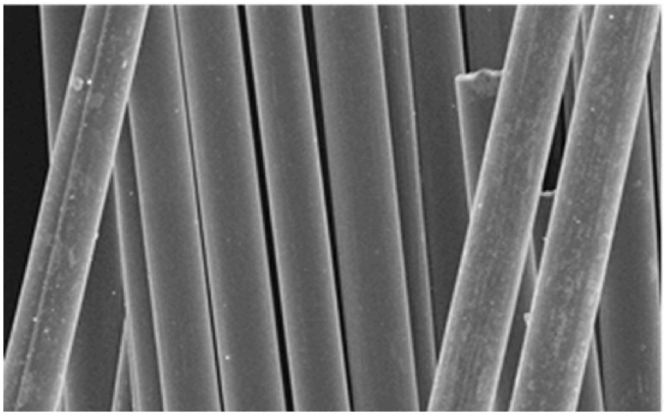

Fig. 2. Fibres' surface characterisation.

variable lengths, a technical datasheet usually does not exist for it. Therefore, some specific characteristics such as diameter distribution, surface quality and tensile strength were determined. The statistical distribution of the diameter (Fig. 1) was assessed by considering a statistical sample of 30 measurements using a LEICA DVM6 optical microscope device. The average diameter was found to be 7.27 ± 0.72 μm.

A Scanning Electron Microscope Zeiss LEO 1530 SEM instrument was used to perform morphological characterisation of the surface of the fibres. Fig. 2 highlights a smooth surface free of carbonaceous deposits due to the relevance of sizing. Lastly, single-filament tensile tests (SFTT) were performed in accordance with ASTM 3379, using a Zwich Roell 1 K dynamometer equipped with a loading cell of 5 N. Samples were set up bonding a single filament on cardboard with 10, 20 and 40 mm gauge lengths, which was then clamped between the tools of the dynamometer. Tensile tests consisted of 30 repetitions for each gauge length and were performed at a constant crosshead rate of 1 mm/min using a preload of 0.002 N. Both tensile modulus and tensile strength were calculated using the nominal value of the fibre's diameter, which was identified beforehand.

The load-extension curves derived from the single fibre tensile test of 30 fibres with gauge lengths of 10, 20 and 40 mm are shown in Fig. 3. The strength data were interpreted with the Weibull statistic, normally adopted to describe the strength distribution of single fibres with the assumption that defects exist (Fu and Lauke, 1998; Garoushi et al., 2006). Both scale (σ_0) and shape (β) parameters, whose values are reported in Table 1, were pinpointed by linearising the cumulative distribution function, as reported in Eq. (1),

$$\ln\left(\ln\left(\frac{1}{1-F}\right)\right) = \beta\ln(\sigma) - \beta\ln(\sigma_0) + \ln(AL_f) \quad (1)$$

where σ is the tensile strength of a single fibre, A the fibre cross section,

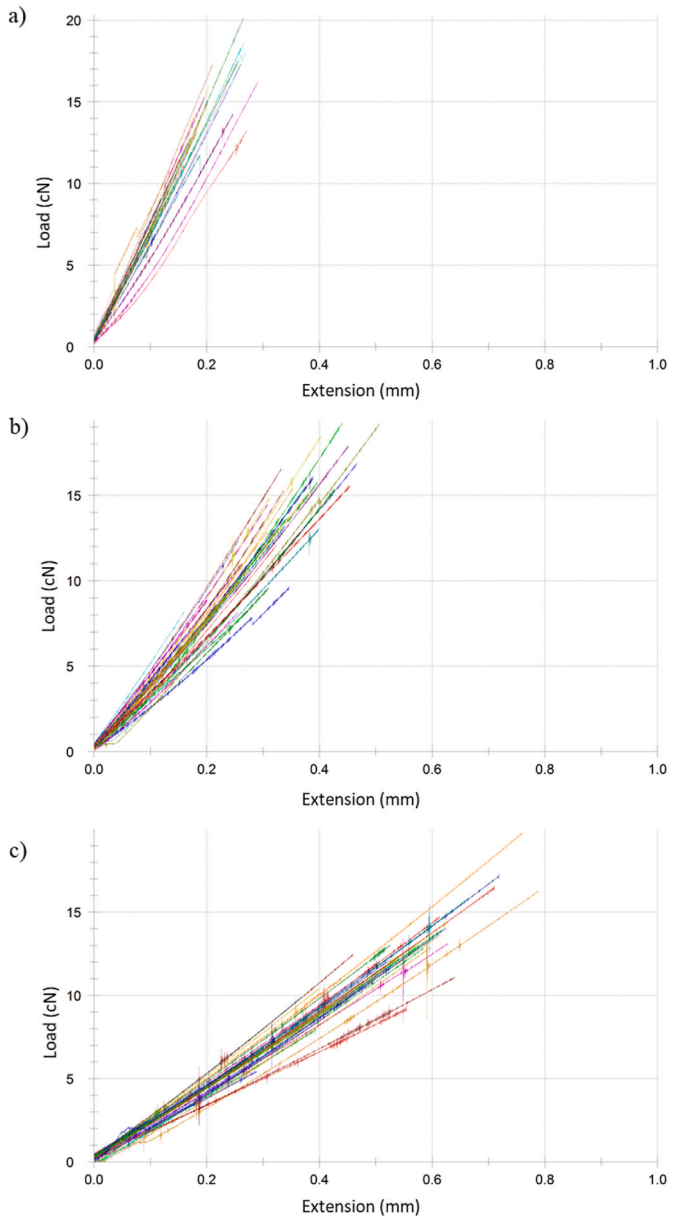

Fig. 3. Load-extension curves for 10 (a), 20 (b) and 40 (c) mm gauge length.

Table 1
Weibull statistics parameters for the rCF used.

Single fibre length	σ_0 (MPa)	β
rCF (10 mm)	3802	5.41
rCF (20 mm)	3601	4.08
rCF (40 mm)	3368	4.70

L_f the gauge length of a single fibre during the test and F the probability of failure.

Specifically, F was obtained by taking experimental data about tensile strength into account following a median-order approach, as shown in Eq. (2) (Davidge, 1978),

$$F = \frac{i - 0.3}{N + 0.4} \quad (2)$$

where i is the i-th stress datum and N the total number of samples. An example of a plot, with its linear fitting procedure, is shown in Fig. 4.

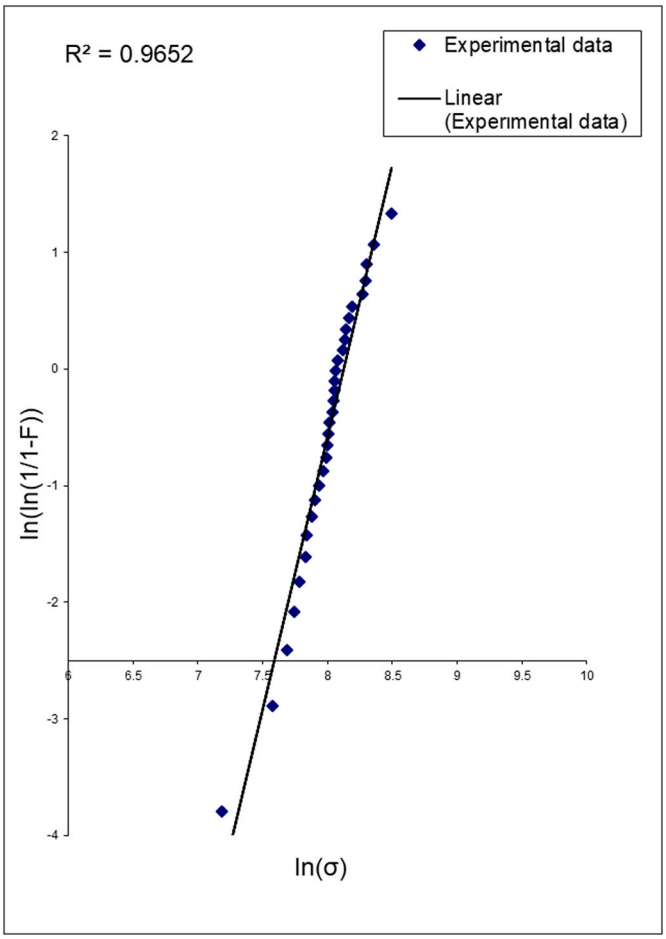

Fig. 4. Weibull linear-fitting plot for 40 mm rCFs.

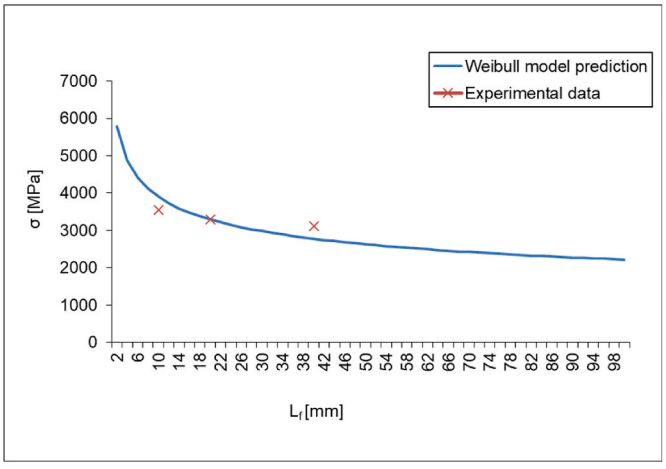

Fig. 5. Tensile strength of the sample used as a function of gauge length (reliability = 50%).

Lastly, the tensile strength was determined by varying the fibre length (L), as the former depends on the latter, considering a specific breaking probability and inverting Eq. (1). Therefore, Eq. (2) becomes Eq. (3):

$$\sigma = \sigma_0 \left(\frac{L_f}{L}\right)^{1/\beta} \tag{3}$$

Fig. 5 shows the graphs drawn from Eq. (3) using the parameters reported in Table 1 and the experimental data obtained following Eq. (2). Overall, it is possible to state that the Weibull model predicts the experimental data very well.

To summarise, the properties of rCF, virgin polyester fibre and virgin polyamide fibre are reported in Table 2.

Table 2
Properties of rCF, polyester (PL) and polyamide (PA) used for manufacturing ring-spun hybrid yarns.

Characteristics	rCF	PL	PA
Fibre diameter (μm)	7.27 ± 0.72	20.1 ± 1.7	18.6 ± 1.5
Single fineness (dtex)	0.46 ± 0.1	3.2 ± 0.1	3.4 ± 0.1
Tensile strength (MPa)	3080 ± 710	423 ± 12	480 ± 23
Young's modulus (GPa)	186 ± 30	3.2 ± 0.18	1.7 ± 0.12
Elongation at break (%)	1.39 ± 0.3	32 ± 5.6	56 ± 7.2
Density (g/cm^3)	1.80	1.38	1.14

3. Methods

3.1. The innovative spinning process

The ISP4rCF, sketched in Fig. 6, consists of the same steps as a traditional spinning process with double carding and drawing. However, it has undergone some adjustments to specific existing machinery, as well as operating parameters, to deal with the brittleness, natural crimp absence and sensitivity to stress typical of CFs (Hengstermann et al., 2016). First, attention was given to the carding machine, since the carding phase plays a central role within the whole spinning process. Specifically, a laboratory long-staple carding machine was chosen to guarantee an extremely gentle carding process on rCFs (Fig. 7). Previously, such innovative laboratory spinning machines were used for spinning short staple fibres, such as cotton and polyester (Chattopadhyay et al., 2002). The clearance between the rollers and their relative speeds are reported in Table 3. Furthermore, a low-density card clothing was applied to the carding machine after different attempts. Details are reported in Table 4. Second.

Since doffer's speed regulation plays a fundamental role in the collection of the web, an inverter was installed on the carding machine to avoid breakages. Despite the measures implemented, the production of rovings that are suitable for yarn production was initially limited to solutions with low rCF concentrations (i.e. less than or equal to 40%) (Colombo et al., 2021a). This implies the impossibility of evaluating yarns with higher rCF concentrations, limiting the field of experimentation to solutions with low rCF contents and, therefore, potentially less efficient technical properties. Accordingly, to obtain yarns with an rCF content of 50% or more by weight, a further revision of the initial processing stages was made. In particular, the speed of the feed roller was modified, as well as the gauge of the drafting unit within the drawing phase (details are reported in Fig. 8). To produce a hybrid yarn, a fibre mass (i.e. rCFs blended with polyester or polyamide) has to be placed on the carding feed conveyer after an opening phase (Fig. 9a). More specifically, polyester and/or polyamide fibres are manually opened and subsequently blended with the rCFs. Thereafter, a double passage is performed on a carding machine to attain a better quality sliver. At the end of the first passage, a card web was obtained (Fig. 9b). Subsequently, such a web is inserted back into the machine to perform the second passage, where the sliver is produced through the coiler. The drawing phase then takes place, thus enabling the production of a thinner sliver with well-distributed and well-oriented fibres (Fig. 10a). To produce the roving, the thinner drafted sliver is passed through the flyer machine (Fig. 10b). The value of the total draft applied in the drawing phase is 4.45. In conclusion, the hybrid yarns are realised with a mini ring spinning frame after setting the parameters (Fig. 11).

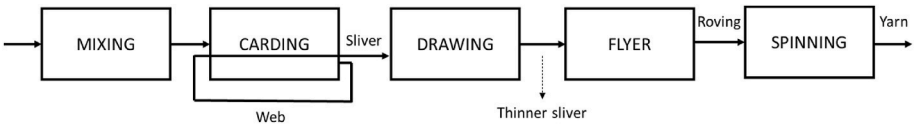

Fig. 6. Steps of the innovative spinning process.

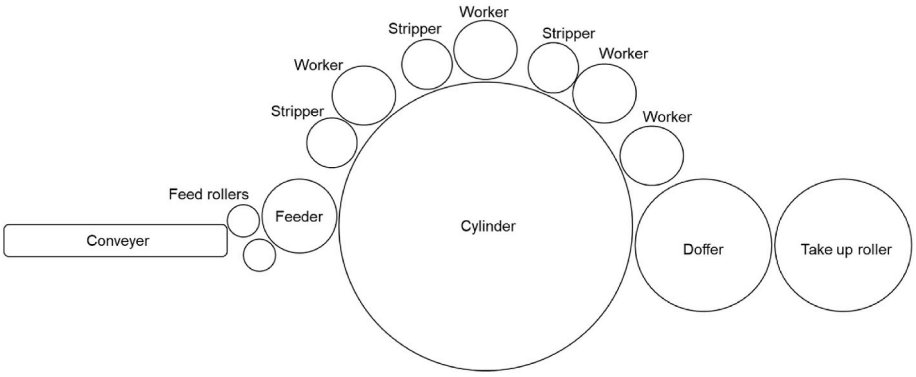

Fig. 7. Basic components (rollers) of the long-staple carding machine used in this study.

Table 3
Clearance between the various rollers and their speed in the carding machine.

Roller	Clearance (mm)	Speed (rpm)
Feeder – Cylinder	0.5	1
1st Worker – Cylinder	0.4	570
1st Stripper – Cylinder	0.4	10
2nd Worker – Cylinder	0.3	570
2nd Stripper–– Cylinder	0.3	10
3rd Worker – Cylinder	0.25	570
3rd Stripper – Cylinder	0.25	10
4th Worker – Cylinder	0.2	950
Cylinder – Doffer	0.2	250 and 12, respectively

Table 4
Card wire features (T: Tooth pitch; α: carding angle).

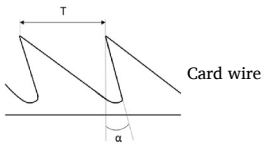

Roller	T (mm)	α (degree)	Tooth density (n. of wires/in^2)
Worker	2.5	35	287
Stripper	3.2	15	224
Feeder	5	20	51
Doffer	2.5	35	287
Cylinder	1.8	20	398

3.2. Production of ring-spun hybrid yarns

In this study, two different blending ratios of rCFs and polyester fibres or polyamide fibres were considered, namely 50–50% and 70–30% by weight. In accordance with the above, rCF concentrations below 50% were not studied, as they were considered responsible for the production of yarns with unsuitable technical properties. Likewise, blends with rCF percentages above 70% were excluded following visual checks. To produce the yarns, the ISP4rCF proposed in Section 3.1 was adopted. More specifically, a 25 g fibre mass (i.e. rCF blended with polyester or polyamide) was placed on a carding feed conveyer for the manufacturing of each card web. The opening and blending phases were performed manually. The sliver was then produced on the carding machine with a coiler. Subsequently, the drawing phase and the flyer machine enabled the roving to be manufactured. Three or 5 slivers were doubled during drawing to increase fibre parallelisation and thus potentially improve the quality of the final yarn. Lastly, the different hybrid yarns were produced with a mini ring spinning frame set to maintain 300 tpm. Table 5 reports the complete spinning plan.

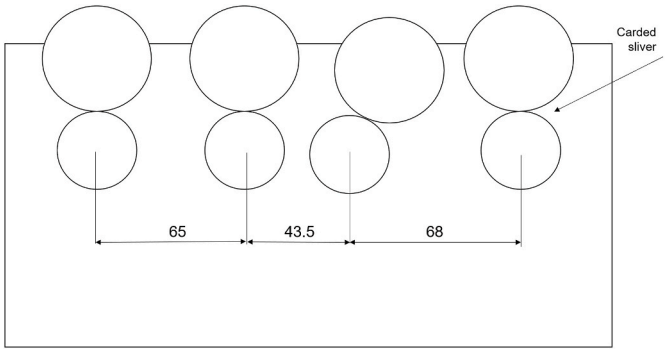

Fig. 8. Clearance between the different drafting groups (values in millimetres).

3.3. Control methods

During the proposed ISP4rCF two kinds of control were performed to validate it and evaluate the range of blends of rCFs that can be processed to obtain ring-spun yarns suitable for the production of CFRPs for structural applications. As reported in Fig. 12, these controls are two visual checks and two final quantitative checks. The control process adopted was 'pass–fail'. Therefore, if a blend failed the first visual check, it was directly discarded without subsequent controls.

3.3.1. Visual controls

Similar to Hengstermann et al. (2016), two consecutive visual controls were conducted to investigate the orientation of CF in semi-finished products. The first check was carried out on the web after the first passage through the carding machine, while the second check was performed on the carded sliver as it exited the coiler. In each inspection, the surface of the semi-finished product was monitored by two experts to determine the absence of any imperfections or holes. Thereafter, owing

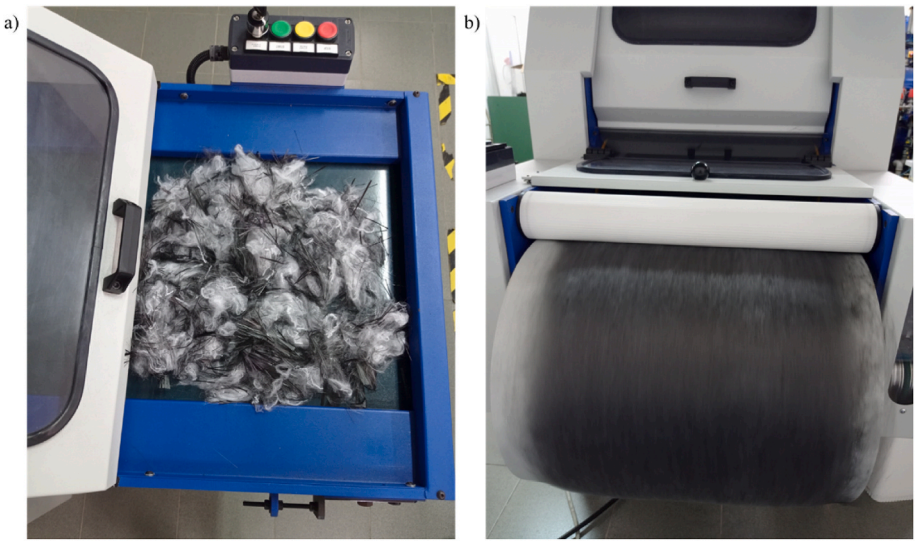

Fig. 9. a) Mixing phase before carding; **b)** Carding machine used in the study.

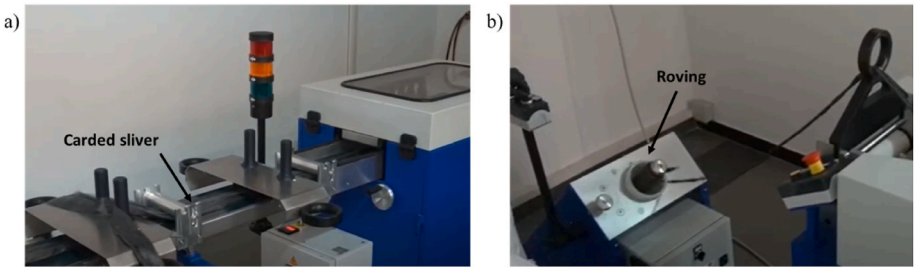

Fig. 10. a) Doubling of the drawing phase; **b)** Flyer machine for the production of the roving.

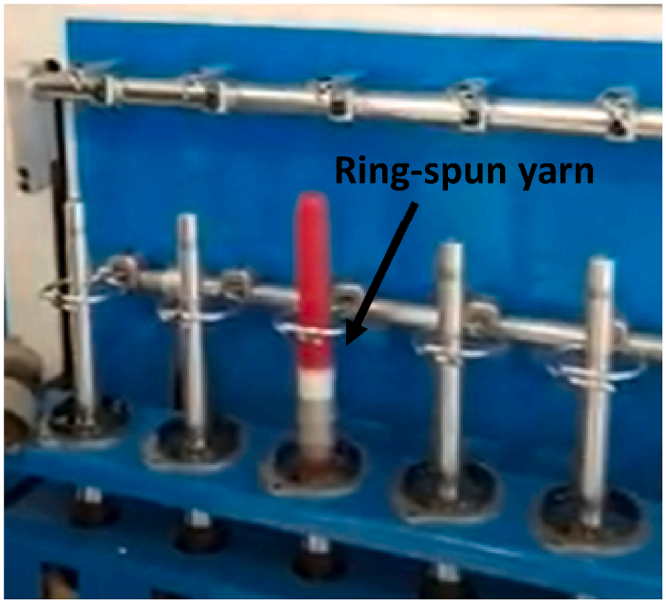

Fig. 11. Ring spinning machine adopted in the study with ring bobbin production.

to the difference in colour of the two fibres used, it was possible to assess both the orientation of the CFs and the homogeneity of the individual outputs.

3.3.2. *Quantitative controls*

Eventually, two quantitative controls were executed. First, the amount of CF remaining in a semi-finished product, namely the roving, was derived through a thermal investigation. Specifically, to remove the thermoplastic fibres without impacting the CF, a specimen of approximately 150 mg per roving was subjected to pyrolysis under nitrogen (Naqvi et al., 2018; Oliveux et al., 2015). The different specimens were weighted to the fifth decimal figure exactly and placed in crucibles. They were then inserted into an oven previously conditioned at 200 °C under nitrogen. A temperature of 500 °C was reached with a ramp of about 20 °C/min. After a standstill of about 45 min, cooling was set (speed below 2 °C/min). At around 300 °C, the nitrogen flow was interrupted, and to ensure a clean surface for CFs, post-oxidation was carried out. Specifically, the temperature was raised to about 450 °C, and the samples were stagnated for 15 min. Finally, they were cooled in the air. The final roving's rCF percentage composition was determined by weighing the residual rCF mass. Second, a series of laboratory tests were conducted to assess the physical, mechanical and thermal properties of the hybrid yarns produced. Such tests are presented below.

3.3.2.1. Count. The mean count of the hybrid yarns was calculated by considering 3 samples whose counts were computed according to the well-known formula for direct *dtex* counting (Eq. (4)):

$$10000 \bullet \frac{P\,(g)}{L\,(m)} \tag{4}$$

where P is the weight in grams of the skein of yarn of length (L) equal to 5 m.

3.3.2.2. Tensile test. Tensile tests of the produced yarns were carried

Table 5
Complete spinning plan.

					Carding	Drawing + Flyer		Spinning
Blend [rCF % first]	Fibre length [mm]	Thermoplastic fibre	#	%rCF	Carded sliver [ktex]	Doubling	Roving [ktex]	Yarn [dtex]
50–50	60	PL	rCF–$PL3_{50}$	50%	1.72	3	1.16	580
	60	PL	rCF–$PL5_{50}$	50%	1.19	5	1.34	447
	60	PA	rCF–$PA3_{50}$	50%	1.90	3	1.28	640
	60	PA	rCF–$PA5_{50}$	50%	1.82	5	2.04	680
70–30	60	PL	rCF–$PL3_{70}$	70%	1.49	3	1.00	501
	60	PL	rCF–$PL5_{70}$	70%	1.33	5	1.50	500
	60	PA	rCF–$PA3_{70}$	70%	1.50	3	1.01	507
	60	PA	rCF–$PA7_{50}$	70%	1.86	5	2.09	695

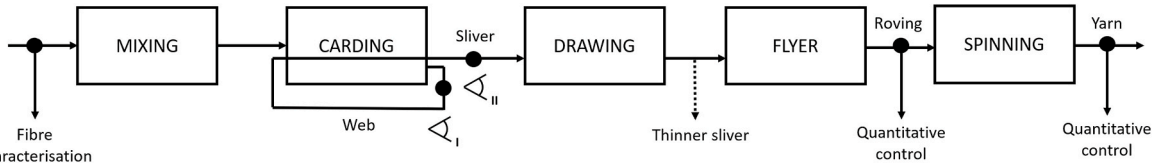

Fig. 12. Control points along the innovative spinning process.

Table 6
Design of experiments – Parameters combinations.

Sample	rCF	Thermoplastic fibre	N. of draw frame doubling
1-9-17	50	PA	3
2-10-18	70	PA	3
3-11-19	50	PA	5
4-12-20	70	PA	5
5-13-21	50	PL	3
6-14-22	70	PL	3
7-15-23	50	PL	5
8-26-24	70	PL	5

out in accordance with ISO 3341 through an MTS ALLIANCE RT50 2 kN dynamometer. For each hybrid yarn, the sample length was set to 500 mm. Specifically, 10 repetitions were performed at a constant crosshead rate of 200 mm/min using flat clamps. Both tensile modulus and tenacity were computed using Testworks®4 software and considered the previously calculated diameter values for each hybrid yarn.

3.3.2.3. Thermogravimetric analysis and differential scanning calorimetry. Thermogravimetric analysis (TGA) and differential scanning calorimetry (DSC) were concurrently carried out using the TA instruments SDT Q600, a simultaneous thermal analyser. TGA was performed to capture at the microlevel the actual number of rCFs present in the hybrid yarns manufactured. DSC was useful for analysing the melting behaviour of the thermoplastic fibres. The weight of the yarn samples entered into the equipment was around 10 mg. As in Maia et al.'s (2019) study, the heating rate of the heat cycle is linear and is set at 10 °C/min until 800 °C is reached from room temperature (25 °C). Three measures for each type of hybrid yarn were carried out. Finally, all samples were tested under nitrogen to ensure an inert environment.

3.3.2.3.1. Plan of experiment. By varying the percentage of recycled CFs, the type of thermoplastic fibre and the number of draw frame doublings on two levels, the experimental campaign was carried out using a 2^3 full factorial design of experiments (DoE). For each combination of parameters, three repetitions were taken into consideration. The full factorial plan illustrating the combination of parameters is shown in Table 6. To examine their potential impact on the amount of recycled CF in the manufactured yarns, an analysis of variance (ANOVA) was performed using Minitab 17[1] software. To do so, a 95% confidence interval was considered.

[1] www.minitab.com/.

Table 7
Blending ratios with findings of the main control points (PL: polyester; PA: polyamide; n.a.: not available; CV: coefficient of variation).

#	Visual control I	Visual control II	Quantitative control [%]	CV [%]
rCF–$PL3_{50}$	Passed	Passed	43.2 ± 1.1	3
rCF–$PL5_{50}$	Passed	Passed	45.2 ± 1.1	2
rCF–$PA3_{50}$	Passed	Passed	48.8 ± 0.8	2
rCF–$PA5_{50}$	Passed	Passed	48.9 ± 0.3	1
rCF–$PL3_{70}$	Passed	Passed	60.8 ± 2.4	4
rCF–$PL5_{70}$	Passed	Passed	65.1 ± 1.3	2
rCF–$PA3_{70}$	Passed	Passed	61.3 ± 0.8	1
rCF–$PA5_{70}$	Passed	Passed	64.3 ± 2.7	4
rCF–$PL3_{80}$	Passed	Not passed	n.a.	n.a.
rCF–$PL5_{80}$	Passed	Not passed	n.a.	n.a.
rCF–$PA3_{80}$	Passed	Not passed	n.a.	n.a.
rCF–$PA5_{80}$	Passed	Not passed	n.a.	n.a.
rCF–$PL3_{90}$	Not passed	n.a.	n.a.	n.a.
rCF–$PL5_{90}$	Not passed	n.a.	n.a.	n.a.
rCF–$PA3_{90}$	Not passed	n.a.	n.a.	n.a.
rCF–$PA5_{90}$	Not passed	n.a.	n.a.	n.a.

4. Results and discussion

4.1. Visual and first quantitative controls

For the production of semi-finished products at an acceptable qualitative level, visual control of the webs and slivers and quantitative control of the rovings were crucial in identifying the range of blends of

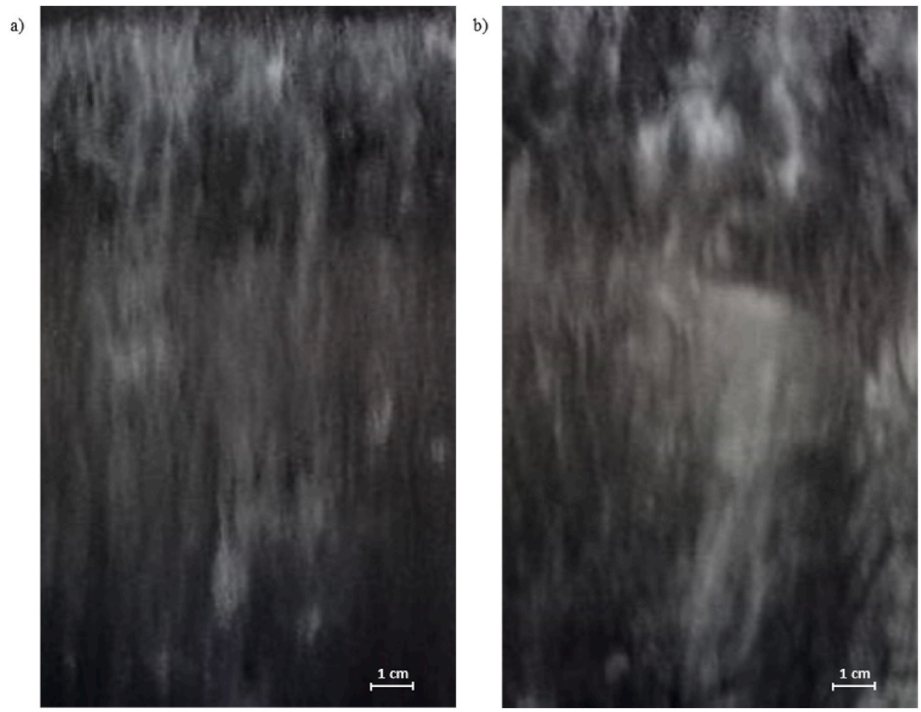

Fig. 13. Fibre orientation in the web **a)** 50-50% rCF and **b)** 70-30% rCF.

rCFs and polyester or polyamide.

Table 7 shows that the workability range of the rCF for the ISP4rCF is between 50% and 70% (for more in-depth information on the replicates of each sample, please refer to Appendix A.1). All blends composed of 50% and 70% rCF passed both visual checks. Moreover, the amount of residual rCFs measured through the quantitative check is higher for 70–30% mixtures. This finding could be considered unsurprising; however, it is essential to capture whether and to what extent each step of the ISP4rCF has an impact on the different blends. Finally, the 90–10% blend did not pass the first visual control, and the 80–20% passed the first visual control but not the second.

Overall, by using rCF percentages within the range of 50%–70%, the mechanical properties and rCF content of the final product should be balanced. On one hand, the higher the mechanical properties of the hybrid yarn, the higher the possibility of obtaining a good-quality reinforcement. On the other hand, the higher the content of rCFs, the higher the mechanical properties of the final composite. Obviously, a quantitative analysis to evaluate the quality of the obtained webs will be essential to optimise the ISP4rCF steps also in the light of a potential industrial-scale transposition.

Additionally, some considerations can be drawn about semi-finished products. From the visual assessment and the numerous observations during the carding phase, it can be claimed that the orientation of the CF in the web and in the carded sliver is better for the 50–50% blends than for 70–30%. As an example, Fig. 13 shows the orientation of the CF for the card web. This finding could be attributed to the fact that clothing applied to the carding machine can better process fibre mixtures where the percentage of CF is lower. Nevertheless, it is currently impossible to predict which CFRPs will have the best mechanical properties because no obvious distinctions can be perceived.

By contrast, quantitative control of rovings shows that, on average, the process impacts all the different blends and slightly more on those with higher CF percentages. It is likely that rCFs are subject to more breakage when they are present in large quantities. Moreover, as the CF reduction is less than 10%, all the rovings produced will be used for the production of ring-spun hybrid yarns that will subsequently be characterised mechanically and thermally and used in the near future for the production of unidirectional thermosetting CFRPs.

Table 8
Values of ring-spun hybrid yarns' counts (σ: standard deviation; CV: coefficient of variation).

#	Mean value [dtex]	σ [dtex]	CV [%]
rCF–$PL3_{50}$	580	53	9
rCF–$PL5_{50}$	447	64	14
rCF–$PA3_{50}$	640	122	19
rCF–$PA5_{50}$	680	40	6
rCF–$PL3_{70}$	501	28	6
rCF–$PL5_{70}$	500	24	5
rCF–$PA3_{70}$	507	26	5
rCF–$PA5_{70}$	695	22	3

4.2. Characterisation of hybrid yarns

4.2.1. Count

Table 8 shows the values of the counts of the different hybrid yarns (for more in-depth information on the replicates of each sample, please refer to Appendix A.2). Three measurements performed on 5 m sample lengths were used. This choice was made in light of the low quantity of ring-spun hybrid yarns produced due to the laboratory scale of the process. Overall, the outcomes exhibited quite high variability values. This could be traced back to the 3 or 4 level of technology readiness (TRL), as the process is innovative. Furthermore, the final spinning machine was configured to maintain a 300 tpm yarn twist. Examining the findings, it appears that the variability for hybrid yarns made up of 70% rCFs is lower than that for yarns composed of 50% rCFs.

Therefore, it can be claimed that the whole ISP4rCF works better for mixtures with higher rCFs percentages. Certainly, once its functionality has been verified, the process will have to be subjected to further improvements in the near future to ensure greater robustness and stability of the final products. In addition, an in-depth analysis of the ends-down will be necessary to assess the efficiency of ring spinning. All these analyses will be indispensable in light of the potential transposition on an industrial scale. An example of ring-spun hybrid yarn is reported in

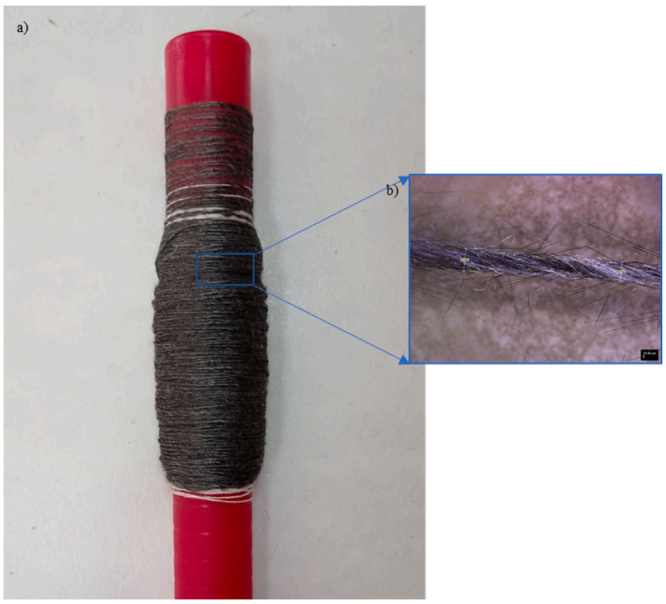

Fig. 14. Hybrid yarns manufactured using 50% rCF and 50% PA3: **a)** yarn bobbin; **b)** optical microscope image.

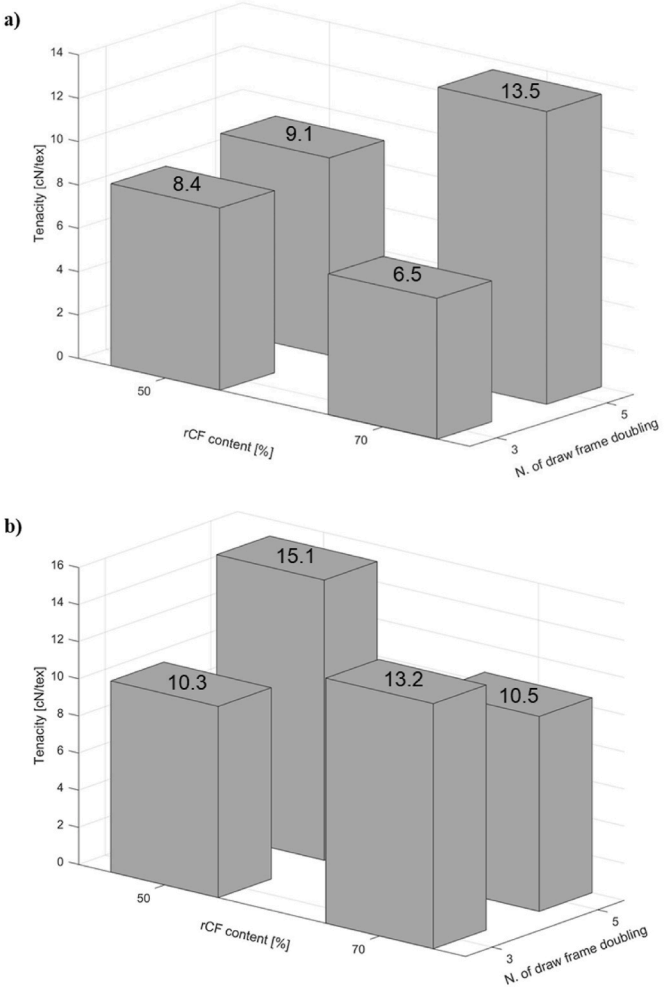

Fig. 15. Tenacity of ring-spun hybrid yarns considering rCF content and number of draw frame doubling for **a)** polyamide and **b)** polyester fibres.

Table 9
Tensile properties of the produced ring-spun hybrid yarns (CV: coefficient of variation).

#	Tenacity [cN/tex]		Strain at break [%]		Young's Modulus [MPa]	
	Mean	CV [%]	Mean	CV [%]	Mean	CV [%]
rCF–$PL3_{50}$	10.3 ± 3.1	30	6.5 ± 0.9	14	917.2 ± 197.4	22
rCF–$PL5_{50}$	15.1 ± 4.8	32	6.6 ± 0.7	11	771.1 ± 149.5	19
rCF–$PA3_{50}$	8.4 ± 2.7	32	13.4 ± 2.0	15	253.5 ± 53.3	21
rCF–$PA5_{50}$	9.1 ± 3.0	33	13.1 ± 2.2	17	278.9 ± 72.7	26
rCF–$PL3_{70}$	13.2 ± 1.2	9	3.2 ± 0.8	25	2353.9 ± 399.5	17
rCF–$PL5_{70}$	10.5 ± 2.0	19	2.7 ± 1.3	48	3050.6 ± 609.0	20
rCF–$PA3_{70}$	6.5 ± 1.4	22	4.0 ± 0.9	23	952.5 ± 395	41
rCF–$PA5_{70}$	13.5 ± 2.4	18	2.0 ± 0.2	10	2348.1 ± 542.5	23

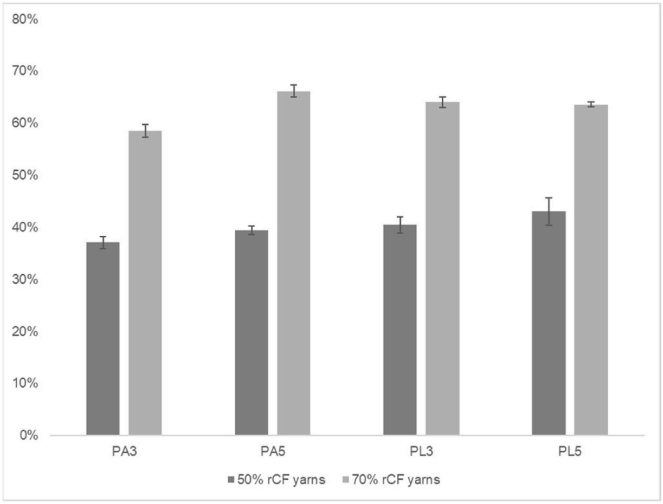

Fig. 16. Share of actual amount of recycled CF for all the hybrid yarns produced measured by TGA (standard deviations are shown as error bars).

Fig. 14.

4.2.2. *Tensile test*

Fig. 15 a) and b) represent the values of tenacity riding on rCF content, number of draw frame doublings and thermoplastic fibre type. It can be claimed that the tenacity of ring-spun hybrid yarns increases when passing from a number of draw frame doubling equal to 3 to 5 for both types of thermoplastic fibres. For instance, when increasing the number of draw frame doublings in the case of 50% rCF, the tenacity rises by 8% and 46% for polyamide and polyester, respectively. The greatest increase (i.e. 108%) occurred in the case of 70% rCF and polyamide. The only exception is represented by the blend composed of 70% rCF and 30% polyester, which shows a decrease of around 26%. Conversely, when examining the values, it cannot be argued that the rCF content increases the tenacity of ring-spun hybrid yarns. This result is not surprising, since with the increasing amount of rCF in the yarn, the possibility for the fibres to slip over each other can increase, thus reducing strength. Moreover, the thermoplastic fibre used could also play a crucial role. Ring-spun hybrid yarns composed of polyester generally showed higher tenacity than those made up of polyamide. This outcome may be attributed to potential reactions occurring between the

Table 10
rCF weight percentage measured by TGA at 750 °C (CV: coefficient of variation).

#	Δ%	CV [%]
rCF–PL3$_{50}$	9.5	8
rCF–PL5$_{50}$	6.9	13
rCF–PA3$_{50}$	12.9	6
rCF–PA5$_{50}$	10.5	4
rCF–PL3$_{70}$	5.9	3
rCF–PL5$_{70}$	6.4	2
rCF–PA3$_{70}$	11.4	4
rCF–PA5$_{70}$	3.8	3

thermoplastic fibre under consideration and the rCF.

Finally, as expected, ring-spun hybrid yarns composed of 70% rCFs are less ductile than those composed of 50% rCFs. Indeed, the former has higher tenacity but lower strain at break than the latter. This outcome is corroborated by the fact that 70% rCF hybrid yarns are characterised by significantly higher Young's modulus values. Therefore, in the case of 70% rCF, breakages occur quite abruptly, likely due to the possibility of the rCF slipping over each other since the number of thermoplastic fibres acting as carriers is lower. As in the study by Hengstermann et al. (2016), no comparisons were made with virgin CF. Indeed, due to the different yarn construction, fibre length and CF content, the results would have limited relevance. The tensile properties of the ring-spun hybrid yarns are listed in Table 9 (For more in-depth information on the replicates of each sample, please refer to Appendix A.3).

4.2.3. Thermogravimetric analysis and differential scanning calorimetry

The results of the TGA (Fig. 16) show a loss of rCFs likely due to one or more of the different steps composing the ISP4rCF. This is particularly true for hybrid yarns composed of 50% rCFs, as they exhibit the highest percentage variation. This outcome corroborates the fact that the whole ISP4rCF seems to have less impact when processing blends with a high amount of rCFs.

Table 10 depicts the percentage reductions for each hybrid yarn (for more in-depth information on the replicates of each sample, please refer to Appendix A.4). The results exhibit that, on average, ring-spun hybrid yarns consisting of higher quantities of rCF are subject to lower reductions. Moreover, when comparing the percentage reduction on rovings with the percentage reduction on hybrid yarns, it can be stated that, in general, the ring spinning stage has less impact on the final amount of rCF than the carding and drafting phases.

Regarding Fig. 16 thoroughly, it can be seen that, irrespective of the kind of thermoplastic fibre, the increase from 3 to 5 draw frame doubling leads to an increase in the percentage of residual rCF in both 50% and 70% yarns. The most significant increase, 13%, occurred in hybrid yarn consisting of 70% rCF and polyamide.

The potential influence of the parameters was statistically confirmed with a three-way ANOVA. The residuals are normally distributed and randomly scattered with an average value close to zero (Fig. 17). Table 11 summarises the p-values obtained. Overall, it

can be observed that the single parameters affect the final amount of rCF after processing; indeed, the low p-values corresponding to each single factor indicate that they are statistically significant. Contrariwise, interactions do not affect it. The high p-values corresponding to the interactions indicate that they are not statistically significant.

According to the data, the best combination for the ring-spun hybrid yarn is 70% rCFs with polyester and 5 as the number of draw frame doublings. This result is also confirmed by the main effects plot shown in Fig. 18.

Fig. 19 illustrates the thermal behaviour of some ring-spun hybrid yarns. The upward and downward curves outline exothermal and endothermal reactions, respectively. In this

investigation, the DSC curves only show downward graphs. Regarding both 50% rCF and 70% rCF yarns, the melting phase takes place at approximately 255 °C for polyester and 260 °C for polyamide.

Table 11
Three-way ANOVA p-values (p-value: ***<0.01, **<0.05, and *<0.1).

Factor	p-value
rCF	0.000***
Thermoplastic fibre	0.046*
N. draw frame doubling	0.018**
rCF*Thermoplastic fibre	0.381
rCF*N. draw frame doubling	0.634
Thermoplastic fibre*N. draw frame doubling	0.104
rCF*Thermoplastic fibre*N. draw frame doubling	0.088*

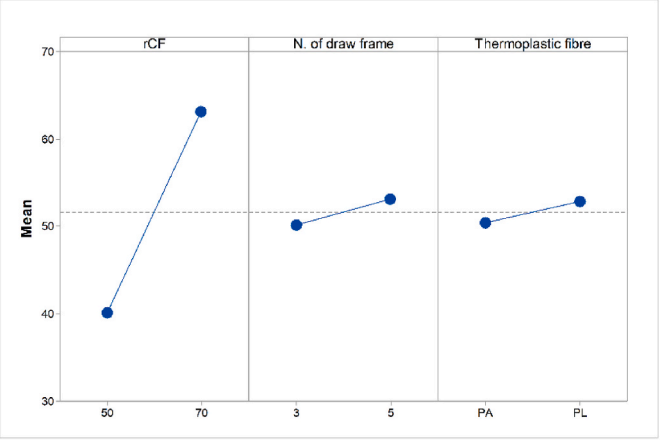

Fig. 18. Main effects plot for output.

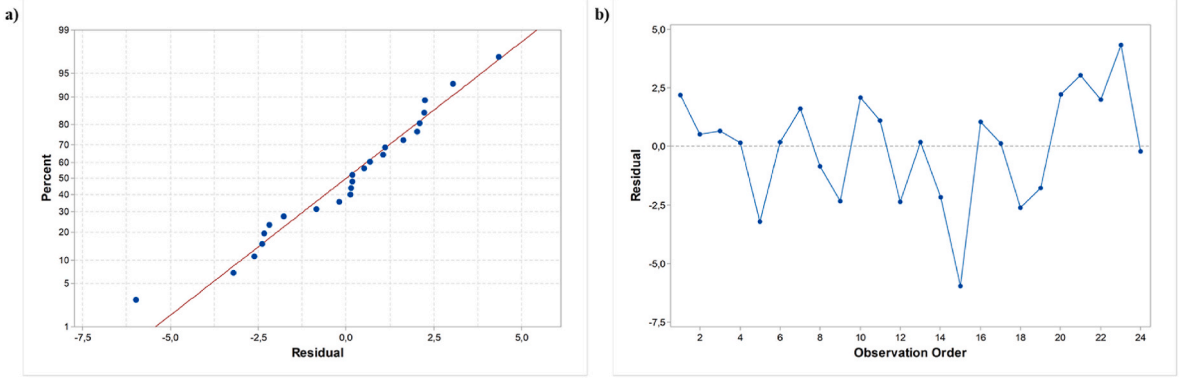

Fig. 17. a) Residual normal distribution and **b)** Randomly scattered residual.

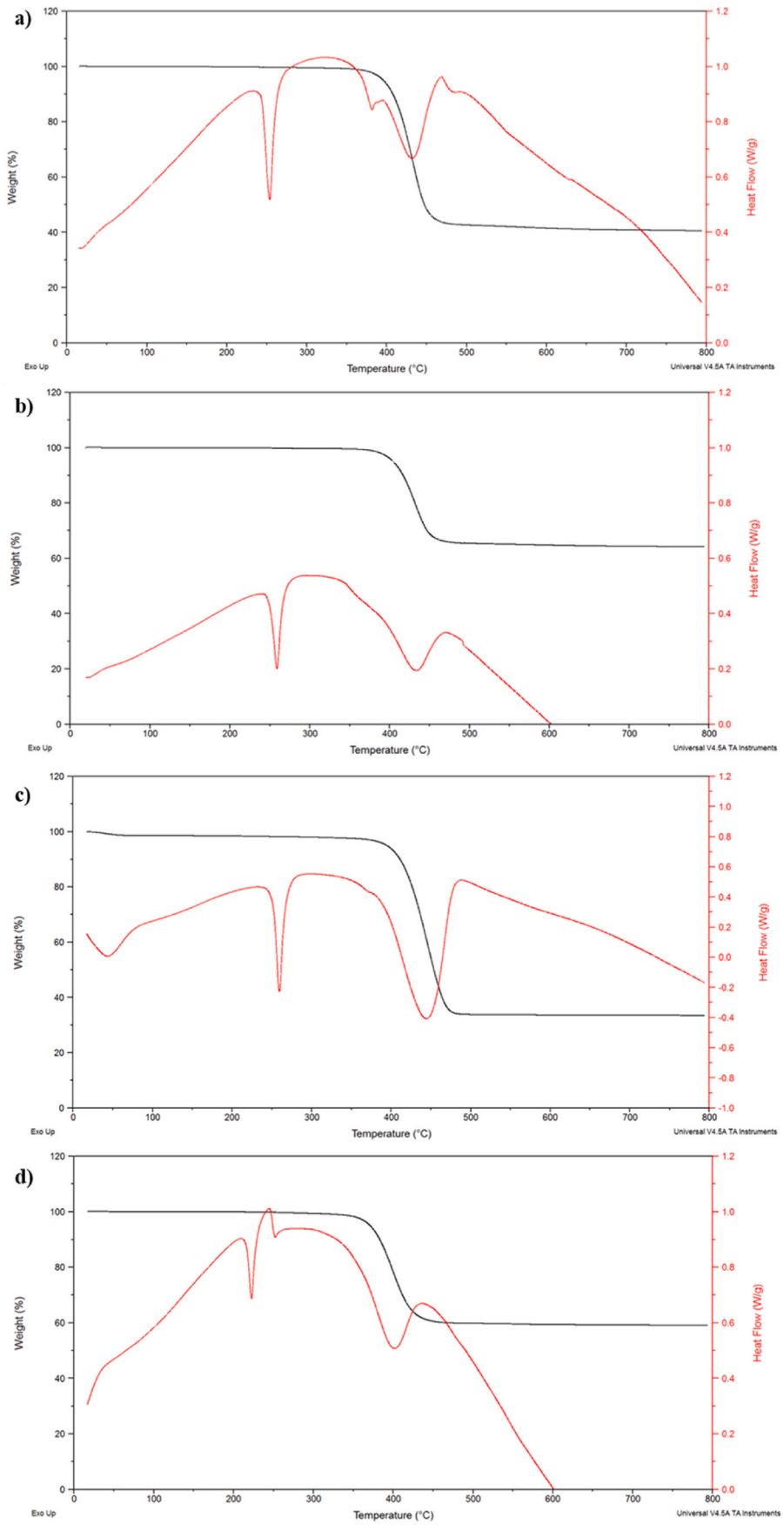

Fig. 19. TGA (black) and DSC (red) curves for hybrid yarn **a)** rCF–$PL3_{50}$, **b)** rCF–$PL3_{70}$, **c)** rCF–$PA3_{50}$, and **d)** rCF–$PA3_{70}$. (For interpretation of the references to colour in this figure legend, the reader is referred to the Web version of this article.)

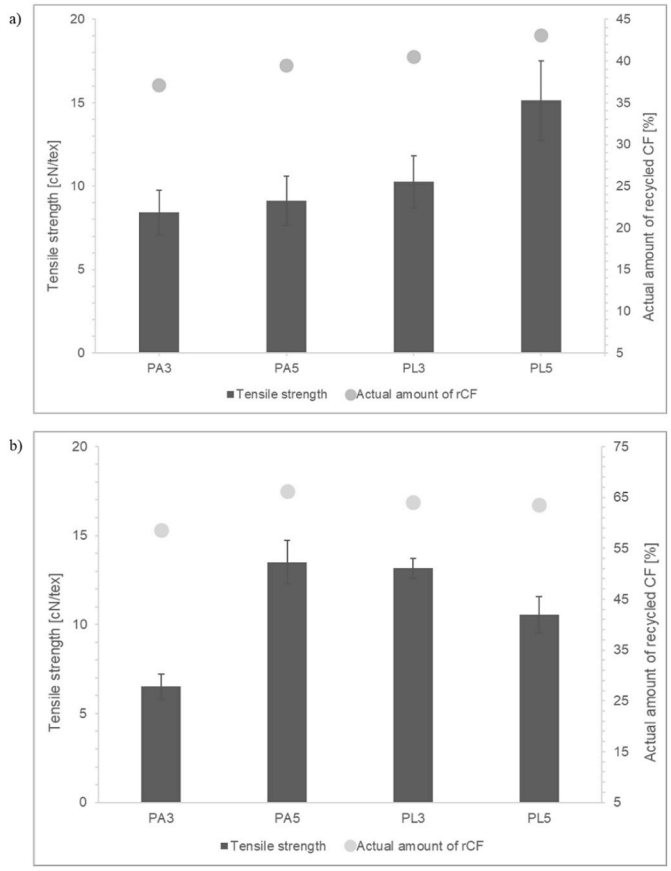

Fig. 20. Tensile strength for the hybrid yarns composed of **a)** 50% rCFs and **b)** 70% rCFs with respect to the real amount of remaining rCFs. The left y-axis represents the tensile strength [cN/tex], while the right y-axis represents the actual remaining rCFs [%] (standard deviations are shown as error bars).

These behaviours are highlighted by the first peak in the corresponding graph. Furthermore, peaks between 400 and 500 °C outline the thermal decomposition of thermoplastic fibres. The decomposition of polyester and polyamide ensures that the TGA curves are constant for temperature values above 500 °C. Moreover, the degradation peak temperature is below 450 °C for all samples; therefore, the values reported in Table 11 (computed at 750 °C) certainly represent the amount of remaining rCFs.

4.2.4. *Tensile strength and TGA values*

Some significant evidence may be drawn by looking at Fig. 20, which depicts the tensile strength of ring-spun hybrid yarns in relation to the actual remaining amount of rCF. The obtained values show that the higher the actual amount of residual rCFs, the higher the tensile strength and vice versa. Overall, regardless of the type of thermoplastic fibre considered, the tensile strength is higher for the hybrid yarns composed of a number of draw frame doubling equal to 5. This finding could be traced back to the fact that, in this case, the drawing phase increases fibre parallelisation to a greater extent. Therefore, the process is gentler with this type of yarn, and the remaining quantity of rCFs is greater.

The only exception is the ring-spun hybrid yarn composed of 70% rCFs and 30% polyester. In this case, the number of rCFs detected decreased slightly as well as the tensile strength. Overall, composites made from ring-spun hybrid yarns consisting of 70% rCF are expected to have the best mechanical and thermal properties and thus better performance.

5. Conclusion

This paper presents an innovative spinning process enabling the production of ring-spun hybrid yarns using rCF from manufacturing scraps blended with virgin polyester or polyamide fibres to increase the application of rCF to more structural components. By adopting a "pass–fail" method, it was found that the range of rCF allowing a good balance between tenacity and the effective amount of rCF of ring-spun hybrid yarns is between 50% and 70%. Thereafter, a comprehensive analysis of ring-spun hybrid yarns consisting of rCFs and virgin polyester or polyamide fibres in 50–50% and 70–30% blending ratios by weight and with a diverse number of draw frame doublings was performed. The findings show that fibre orientation plays a pivotal role, especially for the card web, as does the blending ratio for the whole process. In particular, webs manufactured with 50% rCF have better fibre orientation, as card clothing may better handle lower quantities of rCF. Instead, the tensile tests highlighted that the tenacity of ring-spun hybrid yarns increases when passing the number of draw frame doublings from 3 to 5 for both types of thermoplastic fibres. Further, the increase in rCF content does not significantly affect the tenacity of ring-spun hybrid yarns. Nevertheless, the actual amount of remaining rCF has a strong impact on the tensile strength value. In general, ring-spun hybrid yarns consisting of 70% rCF exhibited slightly higher tensile strength than those consisting of 50% rCF. Moreover, the former suffers from a lower decrease in the quantity of rCFs than the latter. Therefore, it can be stated that ring-spun hybrid yarns composed of 70% rCF, regardless of the type of thermoplastic fibre, have the best mechanical and thermal properties. Accordingly, CFRPs made from this type of ring-spun hybrid yarns are expected to show better performance.

Although results are promising, the ISP4rCF deserves to be improved in terms of robustness and variability. More in detail, to increase its productivity, a specific analysis of the ends-down turns out to be essential.

Overall, it can be claimed that the obtained outcomes open up the possibility of widening the application of circular economy principles to the composite material industry. Nevertheless, to provide first insights into its actual sustainability level, the ISP4rCF should be assessed from an environmental and economic perspective using appropriate tools, such as life cycle assessment and life cycle costing.

Funding

The authors received no financial support for the research, authorship, and/or publication of this article.

CRediT authorship contribution statement

Beatrice Colombo: Conceptualization, Methodology, Formal analysis, Writing – original draft, Writing – review & editing. **Paolo Gaiardelli:** Conceptualization, Methodology, Writing – review & editing. **Stefano Dotti:** Resources, Supervision. **Flavio Caretto:** Resources, Supervision.

Declaration of competing interest

The authors declare that they have no known competing financial interests or personal relationships that could have appeared to influence the work reported in this paper.

Data availability

Data will be made available on request.

Acknowledgments

This paper is part of a research activity carried out within a Ph.D. fellowship entitled "Development of innovative textile architectures based on recycled carbon fibre for the composite materials industry" and funded by ENEA (the Italian National Agency for New Technologies,

Energy and Sustainable Economic Development) in collaboration with Region Lombardy. The authors wish to greatly acknowledge Mrs. Monica Schioppa for performing the TGA and DSC analysis, while Ms. Caterina Blasi and Mr. Giovanni Casciaro for their support, and Mr. Filiberto Valentino for the execution of the tensile tests. Finally, the authors thank Dr. Amelia Montone for the SEM microscope measurements and Dr. Barbara Palazzo for the pyrolysis.

Appendix

Table A1
Residuals values for each roving using pyrolysis from the replicates performed for each sample (σ: standard deviation; CV: coefficient of variation)

#	Values [%]	Mean [%]	σ [%]	CV [%]
rCF–PL3$_{50}$	44.0	43.2	1.1	3
	43.6			
	41.9			
rCF–PL5$_{50}$	44.9	45.2	1.1	2
	44.3			
	46.4			
rCF–PA3$_{50}$	47.9	48.8	0.8	2
	49.6			
	48.8			
rCF–PA5$_{50}$	49.0	48.9	0.3	1
	48.5			
	49.1			
rCF–PL3$_{70}$	58.1	60.8	2.4	4
	62.4			
	61.9			
rCF–PL5$_{70}$	65.8	65.1	1.3	2
	65.8			
	63.6			
rCF–PA3$_{70}$	61.2	61.3	0.8	1
	60.5			
	62.1			
rCF–PA5$_{70}$	67.4	64.3	2.7	4
	62.4			
	63.1			

Table A2
Count values of the ring-spun hybrid yarns from the replicates performed for each sample (σ: standard deviation; CV: coefficient of variation)

#	Count [dtex]	Mean [dtex]	σ [dtex]	CV [%]
rCF–PL3$_{50}$	520	580	53	9
	620			
	600			
rCF–PL5$_{50}$	520	447	64	14
	429			
	400			
rCF–PA3$_{50}$	700	640	122	19
	500			
	720			
rCF–PA5$_{50}$	640	680	40	6
	720			
	680			
rCF–PL3$_{70}$	505	502	28	6
	526			
	472			
rCF–PL5$_{70}$	476	500	24	5
	524			
	498			
rCF–PA3$_{70}$	490	507	26	5
	494			
	537			
rCF–PA5$_{70}$	673	695	22	3
	717			
	697			

Table A3
Tensile properties values of the ring-spun hybrid yarns from the replicates performed for each sample (σ: standard deviation; CV: coefficient of variation)

#	Tenacity [cN/tex]				Strain at break [%]			Young's Modulus [MPa]		
	Value [cN]	Count [tex]	σ	CV [%]	Value [cN]	σ	CV [%]	Value [cN]	σ	CV [%]
rCF–PL3$_{50}$	4.31	58.0	3.1	30	6.39	0.91	14	558.6	197.4	22
	5.26				7.89			836.7		
	5.11				7.18			943.0		
	5.66				6.41			903.3		
	5.32				4.76			938.0		
	8.44				7.07			1085.5		
	8.95				6.91			1231.0		
	7.58				7.09			1125.5		
	4.98				6.24			818.6		
	3.90				5.44			732.0		
rCF–PL5$_{50}$	4.72	44.7	4.8	32	5.70	0.7	11	614.1	149.5	19
	4.88				6.75			581.8		
	5.71				6.96			632.5		
	6.18				6.30			774.7		
	8.17				7.35			857.4		
	10.55				7.52			967.5		
	8.38				6.24			994.5		
	7.51				6.32			864.6		
	4.91				5.39			641.9		
	6.55				7.11			781.7		
rCF–PA3$_{50}$	4.39	64.0	2.7	32	9.35	2.0	15	248.7	53.3	21
	5.43				12.08			243.6		
	4.17				13.38			166.1		
	4.60				13.45			226.7		
	3.98				13.11			193.8		
	6.05				12.65			314.5		
	8.15				16.10			339.9		
	5.05				13.87			296.1		
	4.92				13.68			236.7		
	7.12				16.73			269.2		
rCF–PA5$_{50}$	6.51	68.0	3.0	33	14.41	2.2	17	254.5	72.7	26
	4.71				14.29			189.0		
	3.06				8.99			191.5		
	3.95				10.93			229.0		
	7.50				15.88			240.8		
	5.85				13.24			312.0		
	7.95				12.90			412.5		
	5.33				10.80			274.2		
	8.04				14.20			331.9		
	9.12				15.41			353.4		
rCF–PL3$_{70}$	6.06	50.1	1.2	9	4.25	0.8	25	1939.0	399.5	17
	5.98				4.09			1678.8		
	6.11				3.94			2326.3		
	7.02				3.61			1965.5		
	7.14				3.23			2831.7		
	6.49				3.09			2260.5		
	6.97				2.26			2582.5		
	6.57				3.38			2910.7		
	6.42				2.50			2496.4		
	7.10				2.07			2547.7		
rCF–PL5$_{70}$	6.52	50.0	2.0	19	1.80	1.3	48	3295.7	609.0	20
	6.65				2.40			3795.7		
	4.98				3.62			2919.8		
	4.11				5.88			3047.4		
	5.82				1.40			3762.1		
	5.85				2.10			3012.4		
	5.80				1.90			2113.5		
	4.34				2.60			2223.1		
	3.97				3.21			3719.0		
	4.64				2.11			2616.8		
rCF–PA3$_{70}$	2.64	50.7	1.4	22	4.56	0.9	23	905.9	395.0	41
	4.34				3.08			840.7		
	3.16				2.65			882.5		
	4.43				3.26			1633.8		
	2.69				3.54			440.6		
	3.88				4.88			1655.9		
	3.10				4.27			976.3		
	3.02				5.45			754.1		
	3.40				3.53			799.0		
	2.37				4.37			635.8		
rCF–PA5$_{70}$	10.39	69.5	2.4	18	2.10	0.2	10	1598.6	542.5	23
	8.81				2.04			1943.7		
	9.60				1.63			2992.0		

(*continued on next page*)

Table A3 (*continued*)

#	Tenacity [cN/tex]				Strain at break [%]			Young's Modulus [MPa]		
	Value [cN]	Count [tex]	σ	CV [%]	Value [cN]	σ	CV [%]	Value [cN]	σ	CV [%]
	10.06				1.86			2753.4		
	9.14				2.19			2404.2		
	9.05				2.16			2275.5		
	12.31				2.44			3160.5		
	7.00				1.90			1871.3		
	6.83				2.12			1779.1		
	10.67				1.99			2702.4		

Table A4
Residuals values at 750° of the ring-spun hybrid yarns from the replicates performed for each sample (σ: standard deviation; CV: coefficient of variation)

#	Values [%]	Mean [%]	σ [%]	CV [%]
$rCF-PL3_{50}$	37.3	40.5	3.1	8
	40.7			
	43.5			
$rCF-PL5_{50}$	44.7	43.1	5.4	13
	37.1			
	47.4			
$rCF-PA3_{50}$	39.3	37.1	2.3	6
	34.8			
	37.2			
$rCF-PA5_{50}$	40.1	39.5	1.6	4
	40.6			
	37.7			
$rCF-PL3_{70}$	64.2	64.1	2.1	3
	61.9			
	66.1			
$rCF-PL5_{70}$	62.7	63.6	1.0	2
	64.6			
	63.4			
$rCF-PA3_{70}$	59.1	58.6	2.4	4
	60.7			
	56.0			
$rCF-PA5_{70}$	66.3	66.2	2.3	3
	63.8			
	68.4			

References

Abdkader, A., Hasan, M.M.B., Bachor, S., Cherif, C., 2022. Mechanical properties of composites manufactured from low twist hybrid yarns made of discontinuous carbon and polyamide 6 fibres. J. Thermoplast. Compos. Mater. 0, 1–20. https://doi.org/10.1177/08927057221137800.

Akonda, M.H., El-Dessouky, H.M., Lawrence, C.A., Weager, B.M., 2014. A novel non-crimped thermoplastic fabric prepreg from waste carbon and polyester fibres. J. Compos. Mater. 48, 843–851. https://doi.org/10.1177/0021998313478992.

Akonda, M.H., Lawrence, C.A., Weager, B.M., 2012. Recycled carbon fibre-reinforced polypropylene thermoplastic composites. Composer Part A Appl. Sci. Manuf. 43, 79–86. https://doi.org/10.1016/j.compositesa.2011.09.014.

Bernatas, R., Dagreou, S., Despax-Ferreres, A., Barasinski, A., 2021. Recycling of fiber reinforced composites with a focus on thermoplastic composites. Clean. Eng. Technol. 5 https://doi.org/10.1016/J.CLET.2021.100272.

Chattopadhyay, S.K., Subramanian, R.M., Upadhye, D., 2002. Development of a new miniature spinning system. Asian Textil. J. 11, 84–90.

Clark, E., Bleszynski, M., Valdez, F., Kumosa, M., 2020. Recycling carbon and glass fiber polymer matrix composite waste into cementitious materials. Resour. Conserv. Recycl. 155, 104659 https://doi.org/10.1016/J.RESCONREC.2019.104659.

Colombo, B., Abdoos, A., Gaiardelli, P., Dotti, S., Caretto, F., 2021a. A technical feasibility study of an innovative spinning process for recycled carbon fibres. In: 26th Summer Sch. Fr. Turco, 2021. AIDI-Italian Assoc. Ind. Oper. Profr. 2021.

Colombo, B., Gaiardelli, P., Dotti, S., Caretto, F., 2022. Recycling technologies for fi bre-reinforced plastic composite materials : a bibliometric analysis using a systematic approach. J. Compos. Mater. 0, 1–18. https://doi.org/10.1177/00219983221109877.

Colombo, B., Gaiardelli, P., Dotti, S., Caretto, F., Coletta, G., 2021b. Recycling of waste fiber-reinforced plastic composites: a patent-based analysis, 2021 Recycl 6. https://doi.org/10.3390/RECYCLING6040072. Page 72 6, 72.

Cousins, D.S., Suzuki, Y., Murray, R.E., Samaniuk, J.R., Stebner, A.P., 2019. Recycling glass fiber thermoplastic composites from wind turbine blades. J. Clean. Prod. 209, 1252–1263. https://doi.org/10.1016/j.jclepro.2018.10.286.

Davidge, R., 1978. Mechanical Behavior of Ceramics. Cambridge University Press, Cambridge.

Fernández, A., Santangelo-Muro, M., Fernández-Blázquez, J.P., Lopes, C.S., Molina-Aldareguia, J.M., 2021. Processing and properties of long recycled-carbon-fibre reinforced polypropylene. Compos. B Eng. 211 https://doi.org/10.1016/j.compositesb.2021.108653.

Fu, S.Y., Lauke, B., 1998. The elastic modulus of misaligned short-fiber-reinforced polymers. Compos. Sci. Technol. 58, 389–400. https://doi.org/10.1016/S0266-3538(97)00129-2.

Garoushi, S., Lassila, L., Vallittu, P., 2006. Short fiber reinforced composite: the effect of fiber length and volume fraction. J. Contemp. Dent. Pract. 7, 7–10.

Goergen, C., Schommer, D., Duhovic, M., Mitschang, P., 2020. Deep drawing of organic sheets made of hybrid recycled carbon and thermoplastic polyamide 6 staple fiber yarns. J. Thermoplast. Compos. Mater. 33, 754–778. https://doi.org/10.1177/0892705718811407.

Hasan, M.M.B., Nitsche, S., Abdkader, A., Cherif, C., 2018. Carbon fibre reinforced thermoplastic composites developed from innovative hybrid yarn structures consisting of staple carbon fibres and polyamide 6 fibres. Compos. Sci. Technol. 167, 379–387. https://doi.org/10.1016/j.compscitech.2018.08.030.

Hengstermann, M., Hasan, M., Abdkader, A., Cherif, C., 2017. Development of a new hybrid yarn construction from recycled carbon fibers (rCF) for high-performance composites. Part-II: influence of yarn parameters on tensile properties of composites. Textil. Res. J. 87, 1655–1664. https://doi.org/10.1177/0040517516658511.

Hengstermann, M., Hasan, M.M.B., Scheffler, C., Abdkader, A., Cherif, C., 2021. Development of a new hybrid yarn construction from recycled carbon fibres for high-performance composites. Part III: influence of sizing on textile processing and composite properties. J. Thermoplast. Compos. Mater. 34, 409–430. https://doi.org/10.1177/0892705719847240.

Hengstermann, M., Raithel, N., Abdkader, A., Hasan, M.M.B., Cherif, C., 2016. Development of new hybrid yarn construction from recycled carbon fibers for high

performance composites. Part-I: basic processing of hybrid carbon fiber/polyamide 6 yarn spinning from virgin carbon fiber staple fibers. Textil. Res. J. 86, 1307–1317. https://doi.org/10.1177/0040517515612363.
Khurshid, M.F., Hengstermann, M., Hasan, M.M.B., Abdkader, A., Cherif, C., 2020. Recent developments in the processing of waste carbon fibre for thermoplastic composites – a review. J. Compos. Mater. 54, 1925–1944. https://doi.org/10.1177/0021998319886043.
Lawrence, C.A., 2003. Fundamentals of Spun Yarn Technology.
Lefeuvre, A., Garnier, S., Jacquemin, L., Pillain, B., Sonnemann, G., 2017. Anticipating in-use stocks of carbon fiber reinforced polymers and related waste flows generated by the commercial aeronautical sector until 2050. Resour. Conserv. Recycl. 125, 264–272. https://doi.org/10.1016/j.resconrec.2017.06.023.
Liu, Y., Farnsworth, M., Tiwari, A., 2017. A review of optimisation techniques used in the composite recycling area: state-of-the-art and steps towards a research agenda. J. Clean. Prod. 140, 1775–1781. https://doi.org/10.1016/j.jclepro.2016.08.038.
Longana, M.L., Ong, N., Yu, H., Potter, K.D., 2016. Multiple closed loop recycling of carbon fibre composites with the HiPerDiF (High Performance Discontinuous Fibre) method. Compos. Struct. 153, 271–277. https://doi.org/10.1016/j.compstruct.2016.06.018.
Longana, M.L., Tapper, R.J., Blok, L.G., Hamerton, I., 2021. Recycling of fiber reinforced thermosetting composites. Fiber Reinf. Compos. Const. Compat. Perspect. Appl. 561–595. https://doi.org/10.1016/B978-0-12-821090-1.00018-1.
Maia, B.S., Tjong, J., Sain, M., 2019. Material characterization of recycled and virgin carbon fibers for transportation composites lightweighting. Mater. Today Sustain. 5 https://doi.org/10.1016/J.MTSUST.2019.100011.
May, D., Goergen, C., Friedrich, K., 2021. Multifunctionality of polymer composites based on recycled carbon fibers: a review. Adv. Ind. Eng. Polym. Res. 4, 70–81. https://doi.org/10.1016/j.aiepr.2021.01.001.
Naqvi, S.R., Prabhakara, H.M., Bramer, E.A., Dierkes, W., Akkerman, R., Brem, G., 2018. A critical review on recycling of end-of-life carbon fibre/glass fibre reinforced composites waste using pyrolysis towards a circular economy. Resour. Conserv. Recycl. 136, 118–129. https://doi.org/10.1016/j.resconrec.2018.04.013.
Oliveux, G., Dandy, L.O., Leeke, G.A., 2015. Current status of recycling of fibre reinforced polymers: review of technologies, reuse and resulting properties. Prog. Mater. Sci. https://doi.org/10.1016/j.pmatsci.2015.01.004.
Pakdel, E., Kashi, S., Varley, R., Wang, X., 2020. Recent progress in recycling carbon fibre reinforced composites and dry carbon fibre wastes. Resour. Conserv. Recycl. https://doi.org/10.1016/j.resconrec.2020.105340.
Pickering, S.J., 2006. Recycling technologies for thermoset composite materials-current status. Composer Part A Appl. Sci. Manuf. 37, 1206–1215. https://doi.org/10.1016/j.compositesa.2005.05.030.
Pickering, S.J., Liu, Z., Turner, T.A., Wong, K.H., 2016. Applications for carbon fibre recovered from composites. IOP Conf. Ser. Mater. Sci. Eng. 139 https://doi.org/10.1088/1757-899X/139/1/012005.
Pimenta, S., Pinho, S.T., 2011. Recycling carbon fibre reinforced polymers for structural applications: technology review and market outlook. Waste Manag. 31, 378–392. https://doi.org/10.1016/j.wasman.2010.09.019.
Rademacker, T., 2018. Challenges in CFRP recycling. In: Breaking & Sifting -Expert Exchange on the End-Of-Life of Wind Turbines. Federal Ministry for Economic Affairs and Energy, Germany, pp. 24–25.
Sauer, M., 2019. Composites Market Report 2019-The Global CF-Und CC-Market 2019-Market Developments, Trends, Outlook and Challenges. Carbon Composites: Augsburg, Germany.
Such, M., Ward, C., Potter, K., 2014. Aligned discontinuous fibre composites: a short history. J. Multifunct. Compos. 2, 155–168. https://doi.org/10.12783/issn.2168-4286/2/3/4/such.
Tehrani, M., Boroujeni, A.Y., Hartman, T.B., Haugh, T.P., Case, S.W., Al-Haik, M.S., 2013. Mechanical characterization and impact damage assessment of a woven carbon fiber reinforced carbon nanotube-epoxy composite. Compos. Sci. Technol. 75, 42–48. https://doi.org/10.1016/j.compscitech.2012.12.005.
Tierney, J., Vanarelli, A., Heider, D., Yarlagadda, S., Gillespie, J.W.J., 2019. Aligned Discontinuous Fibre Preforms, Composites and System and Processes of Manufacture. U.S.P. Off. https://doi.org/10.1016/j.ijpe.2012.06.002.
Witik, R.A., Teuscher, R., Michaud, V., Ludwig, C., Månson, J.A.E., 2013. Carbon fibre reinforced composite waste: an environmental assessment of recycling, energy recovery and landfilling. Composer Part A Appl. Sci. Manuf. 49, 89–99. https://doi.org/10.1016/j.compositesa.2013.02.009.
Wölling, J., Schmieg, M., Manis, F., Drechsler, K., 2017. Nonwovens from recycled carbon fibres - comparison of processing technologies. In: Procedia CIRP, pp. 271–276. https://doi.org/10.1016/j.procir.2017.03.281.
Wong, K.H., Turner, T.A., Pickering, S.J., Warrior, N.A., 2010. The potential for fibre alignment in the manufacture of polymer composites from recycled carbon fibre. SAE Int. J. Aerosp. 2, 225–231. https://doi.org/10.4271/2009-01-3237.
Yang, Y., Boom, R., Irion, B., van Heerden, D.J., Kuiper, P., de Wit, H., 2012. Recycling of composite materials. Chem. Eng. Process. Process Intensif. 51, 53–68. https://doi.org/10.1016/j.cep.2011.09.007.
Yao, S.S., Jin, F.L., Rhee, K.Y., Hui, D., Park, S.J., 2018. Recent advances in carbon-fiber-reinforced thermoplastic composites: a review. Compos. B Eng. https://doi.org/10.1016/j.compositesb.2017.12.007.